Label-Free Cancer Cell Separation from Human Whole Blood Using Inertial Microfluidics at Low Shear Stress

ARTICLE *in* ANALYTICAL CHEMISTRY · JUNE 2013

Impact Factor: 5.64 · DOI: 10.1021/ac4006149 · Source: PubMed

5 AUTHORS, INCLUDING:

Joong Ho Shin
Korea Advanced Institute of Science and Tech…

4 PUBLICATIONS **34** CITATIONS

SEE PROFILE

analytical chemistry

Technical Note

pubs.acs.org/ac

Label-Free Cancer Cell Separation from Human Whole Blood Using Inertial Microfluidics at Low Shear Stress

Myung Gwon Lee,[†] Joong Ho Shin,[†] Chae Yun Bae,[†] Sungyoung Choi,[‡] and Je-Kyun Park*[,†,§]

[†]Department of Bio and Brain Engineering, Korea Advanced Institute of Science and Technology (KAIST), 291 Daehak-ro, Yuseong-gu, Daejeon 305-701, Republic of Korea

[‡]Department of Biomedical Engineering, Kyung Hee University, 1732 Deogyeong-daero, Giheung-gu, Yongin-si, Gyeonggi-do 446-701, Republic of Korea

[§]KAIST Institute for the NanoCentury, 291 Daehak-ro, Yuseong-gu, Daejeon 305-701, Republic of Korea

Supporting Information

ABSTRACT: We report a contraction−expansion array (CEA) microchannel device that performs label-free high-throughput separation of cancer cells from whole blood at low Reynolds number (*Re*). The CEA microfluidic device utilizes hydrodynamic field effect for cancer cell separation, two kinds of inertial effects: (1) inertial lift force and (2) Dean flow, which results in label-free size-based separation with high throughput. To avoid cell damages potentially caused by high shear stress in conventional inertial separation techniques, the CEA microfluidic device isolates the cells with low operational *Re*, maintaining high-throughput separation, using nondiluted whole blood samples (hematocrit ~45%). We characterized inertial particle migration and investigated the migration of blood cells and various cancer cells (MCF-7, SK-BR-3, and HCC70) in the CEA microchannel. The separation of cancer cells from whole blood was demonstrated with a cancer cell recovery rate of 99.1%, a blood cell rejection ratio of 88.9%, and a throughput of 1.1×10^8 cells/min. In addition, the blood cell rejection ratio was further improved to 97.3% by a two-step filtration process with two devices connected in series.

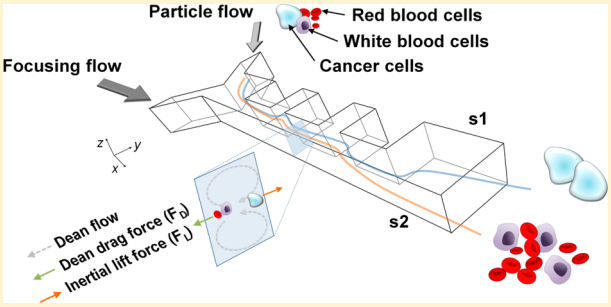

Circulating tumor cells (CTCs) detach from a primary tumor structure and circulate in the blood, spreading to other parts of the body, which is the major cause of metastasis.[1−3] Detection and enumeration of these cells in the early stages of cancer can be used for screening, diagnosis, and prognosis, and isolated cells can also be used to test the efficacy of personalized cancer treatment.[4,5] Although current clinical techniques for isolating CTCs from whole blood are introduced by flow cytometry,[6,7] density gradient centrifugation,[8,9] and immune-affinity capture using magnetic beads,[10,11] these techniques require pretreatment processing of samples, which can cause cell loss and is expensive and labor intensive.

Microfluidics is a well-suited technique for cell separation because of their favorable properties such as low cost, simple procedure, and small amount of space needed and also allows better control of the microenvironment during the cell separation. Immunoaffinity-based capturing approach has been reported for isolation of CTCs with microchips containing microposts and herringbone structures coated with a human epithelial cellular adhesion molecule (EpCAM) antibody.[12,13] Although the device shows effective capturing of CTCs, it must be operated slowly to maintain capture efficiency and the retrieval of viable CTCs is difficult due to the strong binding of cells to the micropost surface. Because the number of CTCs in the blood is very small compared to the number of other blood cells, as small as one CTC per billion blood cells, CTC isolation technique requires high throughput to process blood samples on the milliliter scale with high recovery.[14,15] CTC capturing methods using immunomagnetic nanoparticles demonstrated successful capturing at high throughput.[16] However, such methods require dilution of the blood sample and washing steps, which essentially increase the total volume of the sample that needs to be processed, and possibly cause rare cell loss during the washing steps. Also, to effectively capture rare cells that exist among billions of other blood cells, the amount of magnetic particles required can significantly increase, depending on the amount of blood sample that needs to be treated. Common biological characteristic of CTCs is their diameter (15−30 μm), which is generally larger compared to that of other blood cells (2−15 μm),[17] which gives the possibility of size-based separation. Microfiltering approaches with a cutoff pore size of approximately 8 μm have been demonstrated with a high flow rate and high enrichment concentration, but they may cause clogging of the device and cell damages.[18−21] To overcome the shortcomings of immunoaffinity-based capturing or filtration method to isolate and recover CTCs, a label-free and continuous high-

Received: March 2, 2013
Accepted: June 1, 2013
Published: June 1, 2013

   dx.doi.org/10.1021/ac4006149 | *Anal. Chem.* 2013, 85, 6213−6218

throughput separation technique is needed in the microfluidic separator.

Recent advances in inertial microfluidics using inertial effects such as inertial lift force and Dean flow have allowed the continuous high throughput size-based cell sorting without using external forces.[22] Several inertial separators for isolating cancer cell lines as models of CTCs have been reported in particular geometries such as straight, spiral, and multi orifice structures, using migration differences according to the cell size and cell deformability. In the straight channel, cells being influenced by shear-induced inertial lift force and wall-induced inertial lift force result in distinct equilibrium positions, depending on their size and deformability. Using this mechanism, various cancer cell lines were isolated from diluted blood cells, resulting in a cancer cell recovery rate of over 85%.[23,24] Combination of inertial lift force and Dean flow was used to isolate cancer cells from diluted bloods in a double spiral channel with a recovery rate of ~96% and a blood cell rejection ratio of ~92%.[25] Pinched effect and inertial migration effect on the cells were utilized in a multiorifice array structure for cell focusing, resulting in a cancer cell recovery rate of ~85%.[26] Although previous inertial separators for isolating CTC model cells achieved a high recovery rate (85−97%) and a high throughput (10^4−10^8 cells/min), there is still room for improvement; the blood cell rejection ratio, which determines the isolated CTC purity, is substantially low. Another limitation in the above inertial microfluidic systems is high operational Reynolds number (*Re*) and blood sample dilution step before the injection of the sample to the chip. Most of the inertial separators operate at very high *Re* (*Re* ~30−130), which may cause damage to the cells and affect their viability,[27] and they require additional steps to dilute the whole blood to maintain the separation efficiency.[23−26]

In our previous study, a contraction−expansion array (CEA) microchannel was introduced as a high-throughput inertial separator, utilizing force balance between inertial lift force and Dean drag force.[28−30] The CEA microchannel operates its separation process at a moderate *Re* (~8), without any diluting steps before injection, making it suitable for practical isolation systems of CTCs. In this study, we investigate the various breast cancer cell lines (MCF-7, SK-BR-3, and HCC70) and blood cell migration by force balance differences, and demonstrate cancer cell isolation as a model of CTCs from human whole blood in a single- and double-staged CEA microchannel.

Design Principle. Scheme 1 shows the proposed CEA microchannel for isolating cancer cells from whole blood using inertial effects: (1) inertial lift migration and (2) Dean flow. When the fluid enters into the contraction region, the streamlines from the wider part (expansion region) of the upstream microchannel are accelerated and follow a curved path, producing a similar effect as the Dean flow in a curved microchannel. The particles initially introduced at s1 entrain in the direction of the counter-rotating vortex by Dean flow at each entrance of the contraction region, which results in migration of particles toward s2. The particle migration by Dean drag force ($F_D = 3\pi\mu U_{Dean} a_p$, where μ, U_{Dean}, and a_p are the density of the fluids, transverse velocity by Dean flow and particle diameter, respectively) being induced by Dean flow is dependent on the particle's size and operational flow rate in the fabricated CEA microchannel. On the other hand, throughout the contraction channel, the parabolic nature of a velocity profile makes two kinds of inertial lift force: (1) shear-induced inertial lift force that enables particles to migrate away from the channel center and (2) wall-induced inertial lift force that drives the particles away from the channel wall. By balancing the two different inertial lift forces, the particles thus have two equilibrium positions predicted at ~0.2 times the hydraulic diameter (D_h) away from the sidewalls. The particle migration by inertial lift force ($F_L = \rho U_m^2 a_p^4 C_L / D_h^2$, where ρ, U_m, and C_L are the density of the fluid, *x*-axial maximum flow velocity, and the lift coefficient, respectively) is also dependent on the particle size and operational flow rate in the fabricated CEA microchannel. Under the same condition of flow rate in the fixed dimensional CEA design, the differently sized particles influenced by the force balance ($F_D \propto a_p$, $F_L \propto a_p^4$) have different lateral positions downstream.[28−30]

Scheme 1. Schematic of the Proposed CEA Microchannel for Isolating Cancer Cell from Whole Blood[a]

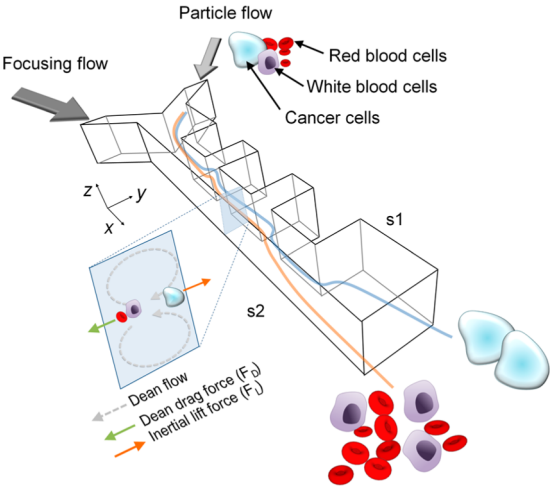

[a]Injected cancer cells and whole blood along s1 of the channel by a focusing flow experience both inertial lift and Dean drag forces. The direction of particle migration is determined by balancing the magnitudes of the two forces, which depend on the cell size. Large-sized cells (cancer cells) dominantly are influenced by the inertial lift force, migrating toward s1, while small-sized cells (red and white blood cells) are dominantly influenced by the Dean drag force, entraining in Dean flow toward s2 (s1: sidewall 1, s2: sidewall 2).

When the cancer cell as a model of CTCs and human whole blood are injected into the particle flow inlet, the cells are influenced by inertial lift force and Dean drag force from opposite directions. Force balance between inertial lift force and dean drag force determines the lateral positions of the injected cells. Large size cells such as cancer cells are dominantly influenced by inertial lift force, migrating toward sidewall 1 (s1), while small size cells such as red blood cells (RBCs) and white blood cells (WBCs) are dominantly influenced by Dean flow, migrating toward sidewall 2 (s2). From this mechanism, the cancer cells as the model of CTCs can be isolated from whole blood.

EXPERIMENTAL SECTION

Microfabrication. The CEA microchannel was 350 μm wide, with 50 μm wide and 1200 μm long contraction regions. The contraction regions were formed with six rectangular structures in the microchannel. The interval between contraction regions was 700 μm. The height of the fabricated CEA microchannel was 63 μm. The CEA microchannel was fabricated in poly(dimethylsiloxane) (PDMS), using soft

dx.doi.org/10.1021/ac4006149 | Anal. Chem. 2013, 85, 6213−6218

lithography techniques. A mixture of PDMS prepolymer and its curing agent (Sylgard 184; Dow Corning, MI) in the ratio of 9:1 was poured on the SU-8 photoresist molds and cured for 3 h in a convection oven at 65 °C. Irreversible bonding was made between a PDMS replica and a glass slide, treating both with an oxygen plasma (200 mTorr, 200 W).

Sample Preparation. To characterize the difference in particle trajectories by their sizes, red fluorescent polystyrene beads of 4, 10, and 15 μm in diameter (Molecular Probes, Eugene, OR) were used for a particle fluid. All beads were prepared in 0.2% Pluronic solution (Sigma–Aldrich), with a concentration of 8.5×10^5, 6.3×10^4, and 5.2×10^4 particles/mL, respectively. We used Pluronic solution to minimize polystyrene beads adhering to the channel wall and with each other. Deionized water was used as a focusing fluid. To demonstrate the cancer cell separation from whole blood and cell migration, we used human whole blood and the breast cancer cell line (MCF-7, SK-BR-3, and HCC70) as a particle fluid, and the phosphate-buffered saline (PBS; Invitrogen Corporation, CA) as a focusing fluid. Before each experiment, whole blood samples were stored at approximately 4 °C to prevent denaturation and cell lysis. The blood samples were obtained from the Republic of Korea National Red Cross Organization (Daejeon, Korea) in compliance with safety regulations. For visualization, the breast cancer cells were stained using a staining reagent (CellTracker Green CMFDA; Molecular Probes, Inc.). The breast cancer cells were treated with ~10 μM CellTracker for ~40 min. The cell permeant reagent was transformed into a cell-impermeant fluorescent solution inside the cells by a glutathione S-transferase-mediated reaction. The breast cancer cells were spiked into the human whole blood diluted with PBS to the ~9%, 23%, and 45% hematocrit level and were injected into the device at each experiment.

RESULTS AND DISCUSSION

Inertial Particle Migration. The inertial migration of the particles of 4, 10, and 15 μm red fluorescent particles was experimentally demonstrated in the CEA microchannel, varying the total flow rate from 3.1 to 12.4 mL/h, corresponding to *Re* of 4.2 to 16.7 (Figure 1). In order to position the microparticles near s1 of the channel, the particles were introduced with a focusing flow and then pushed close to s1. At a *Re* of 8.3, relatively small-sized particles of 4 and 10 μm are pushed toward s2 due to the dominant Dean flow, while large particles of 15 μm occupy their equilibrium position near s1 due to the dominant inertial lift force (Figure 1a).

Under an *Re* of 8.3, because the inertial effects are not enough to be fully developed, regardless of particle size, most of particles maintain their initial position and are observed near s1. However, at a *Re* of 8.3, the particles of 15 μm and 4 and 10 μm are influenced by fully developed inertial effects and migrate toward s1 and s2, respectively. Over a *Re* of 12.6, relatively small particles of 4 and 10 μm begin to migrate toward s2 due to enhancement of inertial lift force, whose magnitude increases with increasing operational flow rate. To determine the optimum flow rate for isolation of cancer cells from blood cells, we calculated the separation resolution (see the Supporting Information) of 10 and 15 μm particles to model the size of WBCs and cancer cells, respectively. From these calculated mean lateral position of 10 and 15 μm particles, separation resolutions were acquired to be 0.42, 0.84, 0.43, and 0.35, corresponding to the total flow rate of 3.1, 6.2, 9.4, and 12.4 mL/h, respectively (Figure 1b). As acquired separation resolution results, we predict that the cancer cells can be isolated from whole blood at a flow rate of ~6.2 mL/h (a *Re* of ~8.3).

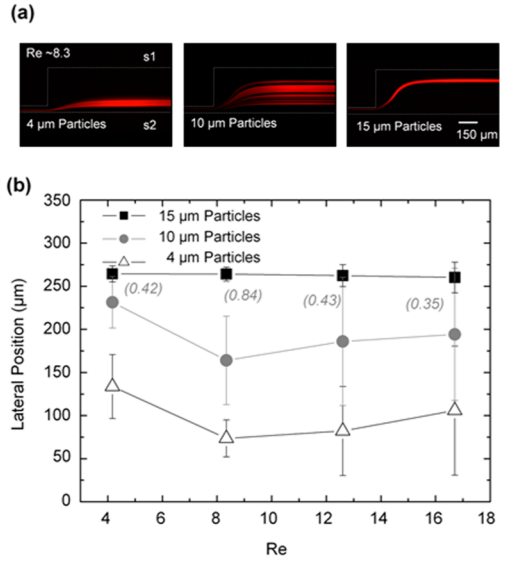

Figure 1. Fluorescence micrograph images of particle migration of 4, 10, and 15 μm red fluorescent particles. (a) The images were obtained at the expansion region after the sixth contraction region. (b) The lateral positions of particles were measured at varying total flow rate (the sum of particle flow rate and focusing flow rate) of 3.1, 6.2, 9.4, and 12.4 mL/h, corresponding to *Re* of 4.2, 8.3, 12.6, and 16.7, respectively. The parentheses denote separation resolution of 10 and 15 μm particles.

Inertial Cell Migration. In order to confirm that the migration mechanism of particles applies to the cell migration, we investigated the cell migration at different *Re* (Figure 2). Compared with the cell sizes between cancer cells and blood cells, the relatively large cells (cancer cells; MCF-7 cells) occupy their own equilibrium position near s1, due to inertial lift force, while relatively small cells (blood cells) migrate toward s2 due to Dean flow especially at a *Re* of 8.1 (Figure 2a). Overall, the mean lateral positions of MCF-7 and blood cells are shifted from s2 to s1 with increased *Re* because the inertial lift force pushing the cells toward s1 is enhanced by an increased flow rate. To determine the optimum flow rate condition for separation of cancer cell from blood cell, we calculated the separation resolution between cancer cell and blood cell and obtained the optimum condition at *Re* = 8.1, corresponding to the total flow rate of 6 mL/h. To investigate the application to other cancer cells, we measured the lateral position of various breast cancer cell lines (HCC70, MCF-7, and SK-BR-3) at different *Re* (Figure 2b). Overall, the trends of lateral position of each cell line are similar, especially over a *Re* of 8.1. All of the cancer cell types are more focused near s1, with increasing *Re* due to the enhancement of the inertial lift force.

Cancer Cell Isolation from Human Whole Blood. To demonstrate the isolation of cancer cells from human whole blood, we redesigned the CEA microchannel with bifurcation outlet and prepared MCF-7 cancer cells spiked into human whole blood (hematocrit level of ~45%) with a final ratio of 1:1000 MCF-7 cells to blood cells. The 1:1000 ratio results in a much greater number of cancer cells compared to that found in clinical samples.[31] However, the ratio was chosen as a proof of

dx.doi.org/10.1021/ac4006149 | *Anal. Chem.* 2013, 85, 6213–6218

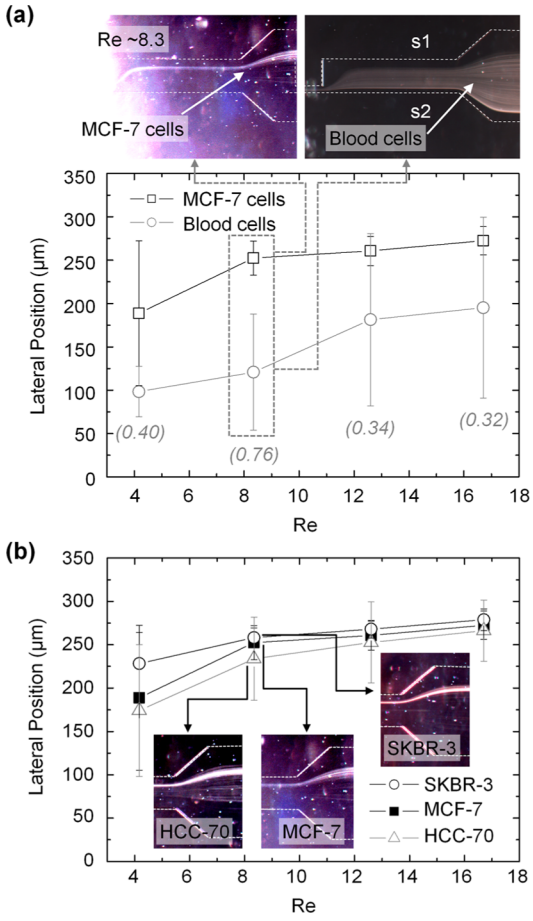

Figure 2. Lateral migration of MCF-7, HCC70, SKBR3, and blood cells at different *Re* of 4.0, 8.1, 12.1, and 16.1, corresponding to a flow rate of 3, 6, 9, and 12 mL/h. (a) Lateral positions of the MCF-7 cell and blood cells were measured and separation resolution between these two cells were calculated with 0.40, 0.76, 0.34, and 0.32, corresponding to *Re* of 4.0, 8.1, 12.1, and 16.1. (b) Lateral positions of other breast cancer cell lines were measured.

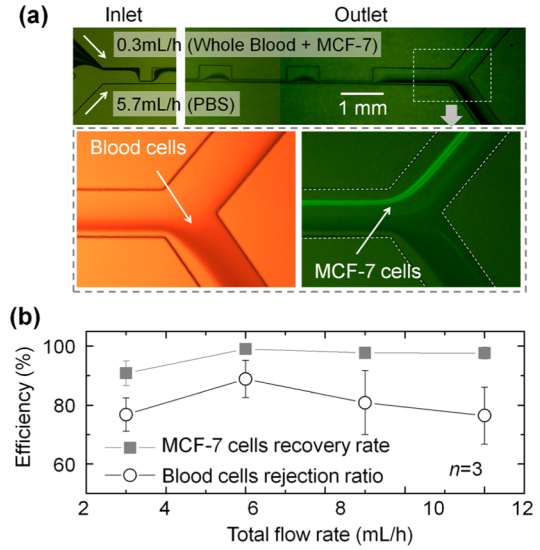

Figure 3. Cancer cell isolation from human whole blood using inertial effect in the CEA microchannel. (a) MCF-7 breast cancer cell as a model of CTCs and human whole blood (hematocrit level of ~45%) were injected into the upper inlet and focused by the focusing flow (PBS buffer) from the bottom inlet at a total flow rate of 6 mL/h. The cancer cells migrated to the upper outlet due to dominant inertial lift force, while the blood cells migrated to the bottom outlet due to the dominant Dean drag force. (b) The separation efficiency: (1) cancer cell recovery rate and the (2) blood cell rejection ratio were calculated to be 90.8%, 99.1%, 97.7%, and 97.7%; 76.8%, 88.8%, 80.8%, and 76.5% at different flow rates of 3, 6, 9, and 12 mL/h, respectively.

concept purpose to show that size-based cell separation using inertial microfluidics is feasible. A large number of cancer cells was used to image all possible trajectories made by a large cell population that include as much variation in cell size as possible. A mixture of the MCF-7 cells and blood cells were introduced with focusing fluid of PBS at a total flow rate of 6 mL/h. In the CEA microchannel, significantly many MCF-7 cells maintain their injected initial position toward the upper outlet and blood cells migrate away from their injected initial position toward bottom outlet (Figure 3a).

In the CTC separation process, the cancer cell recovery rate, blood cell rejection ratio, and throughput are criteria to assess the separation efficiency. The blood cell rejection ratio is the degree at which WBCs and RBCs are excluded from the upper outlet, and it also indicates the purity of the separated cancer cells collected from the upper outlet. For evaluation of performance in the CEA microchannel, separation efficiency was calculated at different flow rates (Figure 3b). Over a total flow rate of 6 mL/h (*Re* ~8.1), where the inertial effect is effective as we already discussed above, cancer cell recovery rates are maintained over 97%. However, the blood cell rejection ratio decreases with an increasing flow rate due to enhancement of inertial lift force that deviates the lateral position of WBCs and RBCs. Especially, at a flow rate of 6 mL/h, the best separation efficiency was achieved with a cancer cell recovery rate, a blood cell rejection ratio, and a throughput of 99.1%, 88.8%, and 1.1 × 10^8 cells/min, respectively. Theoretically, the throughput should be on the order of 10^7 cells/min; however, we calculated the actual throughput by counting the number of cells from the outlets for a known period of time. Cells were collected from both the upper and bottom outlets for 3 min, and then the actual throughput was calculated in terms of number of cells per minute. The syringe that contains the sample was held vertically during the sample injection, causing sedimentation of cells within the syringe and resulting in a throughput which is greater than a theoretical value.

In accordance with the theoretical equations above, the separation efficiency of the cancer cell can be optimized by controlling the magnitude and exposure time of F_D and F_L. Because the particles (or cells) are influenced by inertial lift force throughout the contraction length, we can modulate the exposure time of the inertial lift force on particles (or cells), by changing the contraction region length in the CEA microchannel. In the CEA design with the contraction region shortened by 1/4, cancer cell separation efficiency shows a relatively low recovery rate and high blood cell rejection ratio (Figure S1 of the Supporting Information). Because the most important criterion is high recovery rate in a field of CTC separation considering extremely low abundance of cell number, we selected and demonstrated cancer cell separation in the proposed CEA design with an increased contraction region length. However, further studies of force balances that depend on the design parameter changes of the CEA microchannel are necessary for determining the optimal design to target cells of interest.

dx.doi.org/10.1021/ac4006149 | *Anal. Chem.* 2013, 85, 6213−6218

To apply this separation technique to practical application in the CTC isolation, cell damage is a very important criteria for the retrieval of CTC after an isolation process. Even though inertial separators have been successfully demonstrated cancer cell separation and retrieval with high throughput, there is still potential cell damage by high shear stress induced from a high operational flow rate. However, it is notable that we successfully demonstrated high-performance cancer cell isolation at a low *Re* (~8.1) compared to previously reported inertial cancer cell isolation at high *Re* (~30−130). It is known that cancer cell death proportionally increases with the increasing amount of shear rate and increasing exposure time of the stress,[27] thus it is crucial to minimize both shear rate and exposure time to increase cell viability. An inertial-based approach to enrich cancer cells showed that gene expression and cell viability are not significantly affected by inertial separation at a *Re* of ~21.[23] A comparison of the shear rate in the mentioned device with that in the CEA device, the shear rate is in the same order of magnitude and the exposure time of the stress is an order of magnitude shorter than that in the CEA device, which ensures the cell viability in the CEA device (Figure S2 of the Supporting Information). In addition, because the CEA-based cancer cell isolation performs without a whole blood dilution process before injection, high-throughput isolation can be maintained at a level of 1.1×10^8 cells/min, corresponding to the previous work (10^4−10^8 cells/min).

Improved Cell Separation Using Two-Step Filtration Process. Even though we demonstrated cancer cell separation from whole blood as a model of CTC isolation with high recovery rate and high throughput, there is still a need for enhancing the low blood cell rejection ratio. To improve the blood cell rejection ratio, we redesigned a two-step filtration processing configuration with two CEA parts in the microchannel (Figure S3 of the Supporting Information). Most of injected blood cells were filtered in the first CEA part, and the rest of the blood cells were filtered again in the second CEA part. By this two-step filtration process, we achieved a cancer cell recovery rate of 98.2% and improved the blood cell rejection ratio from 88.9% to 97.4%. The filtered cancer cells in the upper outlet can be collected into a collection tube and applied to a cell culture assay such as a DNA and RNA assay. Although the two-step filtration process shows high separation efficiency, the resistances and pressures within the microchannels, when connected together, become different from those of a single CEA device. Furthermore, upper and lower outlets of a single CEA device both are exposed at atmospheric pressure. However, when the upper outlet of the first CEA device is connected to the upper inlet of the second device, the outlets of the first device are exposed to a different amount of pressure due to the focusing flow 2 of the second device. These are some of the factors to consider during integration of multiple devices and thus optimized operating conditions should be investigated in further studies.

CONCLUSION

We demonstrated label-free size-based inertial separation of cancer cells from whole blood at low shear stress. The cancer separation efficiency was successfully demonstrated and achieved with a throughout of 1.1×10^8 cells/min, a recovery rate of 99.1%, and a blood cell rejection ratio of 88.9%. The device operates at a low *Re* (~8), which causes significantly less shear stress on cells compared to previous works mentioned. Further improved separation efficiency was demonstrated by connecting two CEA microchannel devices in series, which resulted in enhancement of blood cell rejection ratio of 97.4%. In comparison to other inertial separation methods, the CEA separation of the cancer cells from whole blood offers high separation efficiency, less damage to the cells by low shear stress, and a convenient dilution-free process. Although the proposed CEA design has achieved a high blood cell rejection ratio, it is still necessary to improve the blood cell rejection ratio over 99% due to an extremely high abundance of the blood cell number. Also, the size-based cell separation method inherently has limitations due to overlap in the size distribution of WBC and CTC. To overcome such limitations, additional immunoaffinity-based separation techniques are considerable, which would give a high throughput filtration by size-based inertial separation method first and then further separation of CTCs by the immunoaffinity-based separation method. The CEA device's high throughput and effective separation of cancer cells with low damage has potential for improving the diagnosis of cancer and can be contributed to CTC studies and development of point-of-care diagnostics.

ASSOCIATED CONTENT

Supporting Information

Details of measurement setup and analysis, and additional information (Figures S1−S3) as noted in text. This material is available free of charge via the Internet at http://pubs.acs.org.

AUTHOR INFORMATION

Corresponding Author

*E-mail: jekyun@kaist.ac.kr. Tel: +82-42-350-4315. Fax: +82-42-350-4310.

Notes

The authors declare no competing financial interest.

ACKNOWLEDGMENTS

This research was supported by a National Leading Research Laboratory Program (Grant 2011-0018607), a Nano/Bio Science and Technology Program (Grant 2011-0002188), and a Converging Research Center Program (Grant 2011K000864) through the National Research Foundation of Korea, funded by the Ministry of Science, ICT and Future Planning.

REFERENCES

(1) Fehm, T.; Sagalowsky, A.; Clifford, E.; Beitsch, P.; Saboorian, H.; Euhus, D.; Meng, S.; Morrison, L.; Tucker, T.; Lane, N.; Ghadimi, B. M.; Heselmeyer-Haddad, K.; Ried, T.; Rao, C.; Uhr, J. *Clin. Cancer Res.* **2002**, *8*, 2073−2084.

(2) Crnic, I.; Christofori, G. *Int. J. Dev. Biol.* **2004**, *48*, 573−581.

(3) Pantel, K.; Brakenhoff, R. H.; Brandt, B. *Nat. Rev. Cancer* **2008**, *8*, 329−340.

(4) Cristofanilli, M.; Budd, G. T.; Ellis, M. J.; Stopeck, A.; Matera, J.; Miller, M. C.; Reuben, J. M.; Doyle, G. V.; Allard, W. J.; Terstappen, L. W. M. M.; Hayes, D. F. *N. Engl. J. Med.* **2004**, *351*, 781−791.

(5) Al-Mehdi, A.; Tozawa, K.; Fisher, A.; Shientag, L.; Lee, A.; Muschel, R. *Nat. Med.* **2000**, *6*, 100−102.

(6) Moreno, J. G.; O'Hara, S. M.; Gross, S.; Doyle, G.; Fritsche, H.; Gomella, L. G.; Terstappen, L. W. *Urology* **2001**, *58*, 386−392.

(7) Krivacic, R. T.; Ladanyi, A.; Curry, D. N.; Hsieh, H.; Kuhn, P.; Bergsrud, D. E.; Kepros, J. F.; Barbera, T.; Ho, M. Y.; Chen, L. B. *Proc. Natl. Acad. Sci. U.S.A.* **2004**, *101*, 10501−10504.

(8) Baker, M. K.; Mikhitarian, K.; Osta, W.; Callahan, K.; Hoda, R.; Brescia, F.; Kneuper-Hall, R.; Mitas, M.; Cole, D. J.; Gillanders, W. E. *Clin. Cancer Res.* **2003**, *9*, 4865−4871.

(9) Lara, O.; Tong, X.; Zborowski, M.; Chalmers, J. J. *Exp. Hematol.* **2004**, *32*, 891−904.
(10) Allard, W. J.; Matera, J.; Miller, M. C.; Repollet, M.; Connelly, M. C.; Rao, C.; Tibbe, A. G.; Uhr, J. W.; Terstappen, L. W. *Clin. Cancer Res.* **2004**, *10*, 6897−6904.
(11) Riethdorf, S.; Fritsche, H.; Müller, V.; Rau, T.; Schindlbeck, C.; Rack, B.; Janni, W.; Coith, C.; Beck, K.; Jänicke, F. *Clin. Cancer Res.* **2007**, *13*, 920−928.
(12) Nagrath, S.; Sequist, L. V.; Maheswaran, S.; Bell, D. W.; Irimia, D.; Ulkus, L.; Smith, M. R.; Kwak, E. L.; Digumarthy, S.; Muzikansky, A. *Nature* **2007**, *450*, 1235−1239.
(13) Stott, S. L.; Hsu, C.-H.; Tsukrov, D. I.; Yu, M.; Miyamoto, D. T.; Waltman, B. A.; Rothenberg, S. M.; Shah, A. M.; Smas, M. E.; Korir, G. K. *Proc. Natl. Acad. Sci. U.S.A.* **2010**, *107*, 18392−18397.
(14) den Toonder, J. *Lab Chip* **2011**, *11*, 375−377.
(15) Yu, M.; Stott, S.; Toner, M.; Maheswaran, S.; Haber, D. A. *J. Cell Biol.* **2011**, *192*, 373−382.
(16) Hoshino, K.; Huang, Y.-Y.; Lane, N.; Huebschman, M.; Uhr, J. W.; Frenkel, E. P.; Zhang, X. *Lab Chip* **2011**, *11*, 3449−3457.
(17) Meng, S.; Tripathy, D.; Frenkel, E. P.; Shete, S.; Naftalis, E. Z.; Huth, J. F.; Beitsch, P. D.; Leitch, M.; Hoover, S.; Euhus, D. *Clin. Cancer Res.* **2004**, *10*, 8152−8162.
(18) Hu, M.; Huang, M. C.; Cheong, W. C.; Gan, A. T. L.; Looi, X. L.; Leong, S. M.; Koay, E. S.-C.; Li, M.-H. *Lab Chip* **2011**, *11*, 912−920.
(19) Tan, S. J.; Yobas, L.; Lee, G. Y. H.; Ong, C. N.; Lim, C. T. *Biomed. Microdevices* **2009**, *11*, 883−892.
(20) Zheng, S.; Lin, H. K.; Lu, B.; Williams, A.; Datar, R.; Cote, R. J.; Tai, Y.-C. *Biomed. Microdevices* **2011**, *13*, 203−213.
(21) Zheng, S.; Liu, J.-Q.; Tai, Y.-C. *J. Microelectromech. Syst.* **2008**, *17*, 1029−1038.
(22) Di Carlo, D. *Lab Chip* **2009**, *9*, 3038−3046.
(23) Hur, S. C.; Henderson-MacLennan, N. K.; McCabe, E. R.; Di Carlo, D. *Lab Chip* **2011**, *11*, 912−920.
(24) Tanaka, T.; Ishikawa, T.; Numayama-Tsuruta, K.; Imai, Y.; Ueno, H.; Matsuki, N.; Yamaguchi, T. *Lab Chip* **2012**, *12*, 4336−4343.
(25) Sun, J.; Li, M.; Liu, C.; Zhang, Y.; Liu, D.; Liu, W.; Hu, G.; Jiang, X. *Lab Chip* **2012**, *12*, 3952−3960.
(26) Bhagat, A. A. S.; Hou, H. W.; Li, L. D.; Lim, C. T.; Han, J. *Lab Chip* **2011**, *11*, 1870−1878.
(27) Brooks, D. E. *Biorheology* **1984**, *21*, 85−91.
(28) Lee, M. G.; Choi, S.; Park, J.-K. *J. Chromatogr., A* **2011**, *1218*, 4138−4143.
(29) Lee, M. G.; Choi, S.; Park, J.-K. *Appl. Phys. Lett.* **2009**, *95*, 051902.
(30) Lee, M. G.; Choi, S.; Park, J.-K. *Biomed. Microdevices* **2010**, *12*, 1019−1026.
(31) Riethdorf, S.; Fritsche, H.; Müller, V.; Rau, T.; Schindlbeck, C.; Rack, B.; Janni, W.; Coith, C.; Beck, K.; Jänicke, F.; Jackson, S.; Gornet, T.; Cristofanilli, M.; Pantel, K. *Clin. Cancer Res.* **2007**, *13* (3), 920−928.